Ionics (2021) 27:5147–5157
https://doi.org/10.1007/s11581-021-04234-3

ORIGINAL PAPER

Sliding mode-based H-infinity filter for SOC estimation of lithium-ion batteries

Jianxin Yao[1] · Jie Ding[1] · Yanyun Cheng[1] · Liang Feng[1]

Received: 17 May 2021 / Revised: 22 July 2021 / Accepted: 12 August 2021 / Published online: 18 September 2021

Abstract

H-infinity filter (HIf) is widely used in state of charge (SOC) estimation of lithium-ion batteries due to its superior performance to extended Kalman filter (EKF) whose robustness is weak. In this paper, an improved HIf-based SOC estimation algorithm is proposed, which incorporates a sliding mode observer, yielding better estimation stability and accuracy than conventional HIf. The proposed algorithm takes advantages of HIf and sliding mode observer that it is more robust to the modeling error and noises. Samsung ICR18650 lithium-ion battery cell is tested and results show that the proposed method improves SOC estimation accuracy, two error indicators are evaluated and both are reduced compared to that of the EKF and HIf.

Keywords Lithium-ion batteries · H-infinity filter · State of charge · Sliding mode observer

Introduction

Energy crisis and environmental pollution are major problems that have slowed down the development of technology [1]. Because of the merits of long service life, high power rating, high nominal voltage, and excellent safety performance, Lithium-ion batteries (LiBs) have become the most widely used material for storing electrical energy [2]. LiBs reliability, safety and efficiency are determined by the performance of the standard battery management system (BMS) [3]. The state of charge (SOC) is a major factor in BMS and can provide valuable information such as the amount of power left in the LiBs in its current state; thus, effective protection decision can be made to avoid accidents, such as overcharge and overdischarge [4].

However, the SOC of LiBs is unobservable and needs to be estimated based on the characteristics of LiBs [5]. The existing SOC estimation methods can be roughly classified into two groups: non-model-based methods and model-based ones [6]. Non-model type can estimate SOC without constructing a mathematical model that describes the dynamics of LiBs and includes lookup table-based methods and the Coulomb-counting methods. The look-up table-based approach estimates SOC from open circuit voltage (OCV)-SOC relationship table [7]. OCV models are offline methods which require long rests to achieve the desired state [8]. The Coulomb-counting method has good SOC estimation, but it is sensitive to the errors of initial SOC and cumulated during iteration [9, 10].

The mathematical model can also be used to characterize the charging and discharging dynamics of the battery and estimate SOC. There are three well known battery models: data-driven models, electrochemical models and equivalent circuit models (ECM). Data-driven model involves the neural network [11, 12] and fuzzy logic model. They require a large amount of measurements that are precisely detected by high hardware equipment, and models are changing subject to different data set [13–15]. Electrochemical model is the closest to the battery, but due to complex inner chemical reactions, it is difficult to establish a completely appropriate model with desired accuracy [16–18]. The

✉ Jie Ding
dingjie@njupt.edu.cn

Jianxin Yao
1219054120@njupt.edu.cn

Yanyun Cheng
chengyy@njupt.edu.cn

Liang Feng
1218053626@njupt.edu.cn

[1] School of Automation and Artificial Intelligence, Nanjing University of Posts and Telecommunications, Nanjing, 210023, China

computational complexity of the ECM is much smaller than that of the electrochemical model and parameters can be easily estimated by system identification methods. And the ECM does not need a lot of data like what data-driven models do [19–21].

A typical ECM usually utilizes resistor-capacitor (RC) networks to describe the dynamics of LiBs [22, 23]. There are mainly three steps in the ECM-based methods to realize SOC online estimation [24]. Firstly, the relationship between OCV and SOC is fitted by intermittent charge-discharge test or low-current charge-discharge test. Then, an appropriate equivalent circuit model is established with highly estimated model parameters identified by the least square algorithm or other identification algorithms. Finally, the SOC is estimated online by effective methods, but is not limited to proportional-integral-differential (PID) observer [25], sliding mode observer [26], Kalman filter-based algorithms [27–30], H-infinity filter (HIf) [31, 32] and particle filter [33].

A suitable modeling and estimation algorithm with high accuracy is expected in the model-based estimation. Wei et al. [34] integrated recursive total least squares with an SOC observer to reduce the noise impact in SOC estimation of LiBs. Chen et al. [35] employed parameter backtracking strategy in recursive least squares (RLS) to identify the ECM parameters, and applied EKF to estimate the SOC. Luo et al. [36] evaluated the estimation accuracy of SOC by combining a fractional order ECM with cubature Kalman filter. Lao et al. [37] presented a RLS with varying forgetting factor and unscented Kalman filter to identify parameters and estimate SOC online at different temperatures. However, EKF assumes that the noise is white gaussian which is not the case in the real working conditions and will give rise to poor estimation robustness [38].

Since the accuracy of the extended Kalman filter relies greatly on the system model and statistical characteristics of the noises, this paper adopts HIf improved by discrete sliding mode observer (DSMO) to estimate SOC. Sliding mode observer is a kind of nonlinear observer with small calculation amount and good robustness, which reduces the influence of system parameter changes and disturbance to a certain extent [39, 40].

In this article, the RLS method with a forgetting factor (FFRLS) algorithm is utilized for online parameter identification of constructed battery ECM. Further, a modified HIf is established to estimate the SOC of LiBs, where DSMO is used to improve the estimation process. Finally, the performance is tested with data sets from Samsung 18650 LiBs at the process of intermittent discharge and dynamic stress test (DST) with different evaluation methods.

This paper is briefly organized as follows. In "ECM for lithium-ion batteries", an ECM of the battery is constructed, and the online model identification by FFRLS is presented. In "Improved H-infinity filter for SOC estimation", an HIf incorporated with discrete sliding mode observer is presented, and the estimation accuracy SOC is verified by comparison to existing filters under DST in "Experiments and analysis". "Conclusions" summarizes the main work.

ECM for lithium-ion batteries

Lithium-ion battery model

A reliable battery model is primary to accurately estimate the SOC [41]. The dual polarization model shown in Fig. 1 is one of the estimation models with high precision and low computation, which involves three parts: (1) U_{oc} is the open circuit voltage of the power battery; (2) Ohmic resistance R_0 refers to the resistance of power battery electrode materials, electrolyte and other parts; (3) Parallel RC networks, R_a, C_a, R_b and C_b describe the dynamics of LiBs.

According to Kirchhoff's voltage and current law, the state space model of the dual polarization model can be expressed as:

$$\begin{cases} \dot{U}_a = \dfrac{-U_a}{R_a C_a} + \dfrac{I_L}{C_a}, \\ \dot{U}_b = \dfrac{-U_b}{R_b C_b} + \dfrac{I_L}{C_b}, \\ U_L = U_{oc} - U_a - U_b - I_L R_0, \end{cases} \tag{1}$$

where I_L and U_L are the current and terminal voltage of the LiB, respectively, U_{oc} represents OCV. The relationship between OCV and SOC can be fitted by high-order polynomial

$$U_{oc}(s) = \sum_{i=0}^{m} \beta_i SOC^i \tag{2}$$

where β_0 to β_m are the coefficients that can be determined by OCV-SOC test, m is the order of the polynomial that larger m means higher accuracy and robustness in general [42], SOC represents state of charge:

$$SOC(t_1) = SOC(t_0) - \frac{\int_{t_0}^{t_1} \eta i(t) dt}{Q_n} \tag{3}$$

where $SOC(t_1)$ represents the SOC at time t_1, η is the Coulomb coefficient, Q_n is capacity and $i(t)$ is the current, which is positive (negative) when it is discharging (charging).

Parameters estimation

The model in Eq. (1) can be rewritten as

$$U_L(s) - U_{oc}(s) = -I(s)\left(R_0 + \frac{R_a}{1 + R_a C_a s} + \frac{R_b}{1 + R_b C_b s}\right) \tag{4}$$

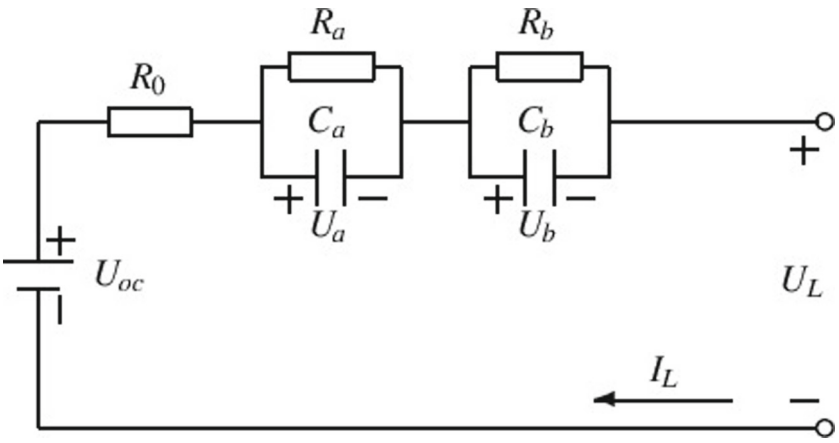

Fig. 1 The second-order RC ECM

Defining $E_L(s) = U_L(s) - U_{oc}(s)$ gives

$$G(s) = \frac{E_L(s)}{I_L(s)} = -\frac{R_0 s^2 + \frac{R_0R_aC_a+R_0R_bC_b}{R_aC_aR_bC_b}s + \frac{R_0+R_a+R_b}{R_aC_aR_bC_b}}{s^2 + \frac{R_aC_a+R_bC_b}{R_aC_aR_bC_b}s + \frac{1}{R_aC_aR_bC_b}} \tag{5}$$

By a bilinear transformation $s = \frac{2}{T}\cdot\frac{1-z^{-1}}{1+z^{-1}}$, where z is the discretization operator and T is the system sampling period, $G(s)$ can be written as:

$$G(z^{-1}) = \frac{E_L(z^{-1})}{I_L(z^{-1})} = \frac{\theta_3 + \theta_4 z^{-1} + \theta_5 z^{-2}}{1 - \theta_1 z^{-1} - \theta_2 z^{-2}} \tag{6}$$

θ_i $(i = 1, 2, \cdots, 5)$ are the coefficients:

$$\begin{cases} \theta_1 = \dfrac{8b - 2T^2}{4b + 2cT + T^2}, \\ \theta_2 = \dfrac{4cT}{4b + 2cT + T^2} - 1, \\ \theta_3 = -\dfrac{4ab + 2eT + dT^2}{4b + 2cT + T^2}, \\ \theta_4 = \dfrac{8ab - 2dT^2}{4b + 2cT + T^2}, \\ \theta_5 = -\dfrac{4ab - 2eT + dT^2}{4b + 2cT + T^2}, \end{cases} \tag{7}$$

where $a = R_0$, $b = \tau_a\tau_b$, $c = \tau_a + \tau_b$, $d = R_0 + R_a + R_b$, and $e = R_0(\tau_a + \tau_b) + R_a\tau_b + R_b\tau_a$, τ_a is R_aC_a, and τ_b is R_bC_b.

Transforming Eq. (6) to obtain a discretized recursive form of the equivalent circuit model,

$$\begin{aligned} E(k) &= \theta_1 E(k-1) + \theta_2 E(k-2) + \theta_3 I(k) + \theta_4 I(k-1) \\ &\quad + \theta_5 I(k-2) \\ &= \boldsymbol{\theta}^{\mathrm{T}}(k)\boldsymbol{\varphi}(k) \end{aligned} \tag{8}$$

where $\boldsymbol{\theta}(k) = [\theta_1 \quad \theta_2 \quad \theta_3 \quad \theta_4 \quad \theta_5]^{\mathrm{T}}$ and $\boldsymbol{\varphi}(k) = [E(k-1) \quad E(k-2) \quad I(k) \quad I(k-1) \quad I(k-2)]^{\mathrm{T}}$, Taking $\hat{\theta}_i(k)$ as the estimates of true $\theta_i(k)$, $i = 1, \cdots, 5$. In order to ensure the uniqueness of the reconciliation, τ_a and τ_b are computed from $\tau_a\tau_b = b$ and $\tau_a + \tau_b = c$, where τ_a takes the maximum value and τ_b takes the minimum.

$$\begin{cases} a = \dfrac{\hat{\theta}_4 - \hat{\theta}_3 - \hat{\theta}_5}{1 + \hat{\theta}_1 - \hat{\theta}_2}, \\ b = \dfrac{T^2(1 + \hat{\theta}_1 - \hat{\theta}_2}{4(1 - \hat{\theta}_1 - \hat{\theta}_2)}, \\ c = \dfrac{T(1 + \hat{\theta}_2)}{1 - \hat{\theta}_1 - \hat{\theta}_2}, \\ d = \dfrac{-\hat{\theta}_3 - \hat{\theta}_4 - \hat{\theta}_5}{1 - \hat{\theta}_1 - \hat{\theta}_2}, \\ e = \dfrac{T(\hat{\theta}_5 - \hat{\theta}_3)}{1 - \hat{\theta}_1 - \hat{\theta}_2}, \end{cases} \tag{9}$$

$$\tau_a = \frac{c + \sqrt{c^2 - 4b}}{2}, \tau_b = \frac{c - \sqrt{c^2 - 4b}}{2} \tag{10}$$

Thus the resistance and capacitance of the ECM can be obtained:

$$\begin{cases} R_0 = a, \\ R_a = [\tau_a(d - a) + ac - e]/(\tau_a - \tau_b), \\ R_b = d - a - R_a, \\ C_a = \tau_a/R_a, \\ C_b = \tau_b/R_b, \end{cases} \tag{11}$$

Recursive least squares method can realize online identification, but as the amount of data increases during the recursive process, too much old data will decrease the convergence rate. To tackle this issue, FFRLS [43, 44] identification algorithm is employed which can identify the dynamic model parameters online, and accelerate the estimation speed by a forgetting factor. The main steps of FFRLS are referred to Ref. [45].

Improved H-infinity filter for SOC estimation

Dual polarization model linearization

As shown in Fig. 1, the voltages of the two RC links under Dual polarization model excitation are:

$$\begin{cases} U_{a,k} = U_{a,k-1}e^{-\frac{\Delta t}{\tau_a}} + [1 - e^{-\frac{\Delta t}{\tau_a}}]i_{L,k}R_a, \\ U_{b,k} = U_{b,k-1}e^{-\frac{\Delta t}{\tau_b}} + [1 - e^{-\frac{\Delta t}{\tau_b}}]i_{L,k}R_b, \end{cases} \tag{12}$$

where $U_{a,k}$ and $U_{b,k}$ are voltages of the RC link a and b at time k, respectively, $i_{L,k}R_a$ and $i_{L,k}R_b$ represents the final steady-state voltages of RC link a and b. We have

$$U_L = U_{oc} - U_a - U_b - IR_0 \tag{13}$$

By discretization of Eqs. (3), (12) and (13), the following model can be derived:

$$\begin{pmatrix} U_a(k+1) \\ U_b(k+1) \\ SOC(k+1) \end{pmatrix} = \begin{pmatrix} e^{-\frac{T}{\tau_a}} & 0 & 0 \\ 0 & e^{-\frac{T}{\tau_b}} & 0 \\ 0 & 0 & 1 \end{pmatrix} \begin{pmatrix} U_a(k) \\ U_b(k) \\ SOC(k) \end{pmatrix} + \begin{pmatrix} R_a(11-e^{-\frac{T}{\tau_a}}) \\ R_b(1-e^{-\frac{T}{\tau_b}}) \\ -\frac{\eta T}{Q_n} \end{pmatrix} I(k) + \boldsymbol{\omega}(k) \tag{14}$$

$$U_L(k) = \begin{pmatrix} -1 & -1 & \frac{\partial U_{oc}}{\partial SOC} \end{pmatrix} \begin{pmatrix} U_a(k) \\ U_b(k) \\ SOC(k) \end{pmatrix} - R_0 I(k) + \nu(k) \tag{15}$$

where $\boldsymbol{\omega}(k)$ and $\nu(k)$ are process noise and measurement noise, respectively, and

$$\begin{aligned} \boldsymbol{A}_k &= \begin{pmatrix} e^{-\frac{T}{\tau_a}} & 0 & 0 \\ 0 & e^{-\frac{T}{\tau_b}} & 0 \\ 0 & 0 & 1 \end{pmatrix} \\ \boldsymbol{B}_k &= \begin{pmatrix} R_a(1-e^{-\frac{T}{\tau_a}}) \\ R_b(1-e^{-\frac{T}{\tau_b}}) \\ -\frac{\eta T}{Q_n} \end{pmatrix} \\ \boldsymbol{C}_k &= \begin{pmatrix} -1 & -1 & \frac{\partial U_{oc}}{\partial SOC} \end{pmatrix}, \quad D_k = -R_0 \end{aligned} \tag{16}$$

Then, the model in Eqs. (14)–(15) can be simplified as follows:

$$\begin{cases} \boldsymbol{x}_k = \boldsymbol{A}_{k-1} \cdot \boldsymbol{x}_{k-1} + \boldsymbol{B}_{k-1} \cdot u_{k-1} + \boldsymbol{\omega}_{k-1} \\ y_k = \boldsymbol{C}_k \cdot \boldsymbol{x}_k + \boldsymbol{D}_k \cdot u_k + \nu_k \end{cases} \tag{17}$$

where $\boldsymbol{x}_k = [U_a(k),\ U_b(k),\ SOC(k)]^{\mathrm{T}}$, $u_{k-1} = I(k-1)$, $y_k = U_L(k)$.

H-infinity filter

Because EKF can only estimate SOC under Gaussian white noise with limited accuracy, H-infinite filter for SOC estimation is proposed to overcome the problems encountered by Kalman filter and obtain higher estimation accuracy and better robustness. The standard linear time-varying discrete system is as follows:

$$\begin{cases} \boldsymbol{x}_k = \boldsymbol{A}_{k-1} \cdot \boldsymbol{x}_{k-1} + \boldsymbol{B}_{k-1} \cdot u_{k-1} + \boldsymbol{\omega}_{k-1}, \\ y_k = \boldsymbol{C}_k \cdot \boldsymbol{x}_k + \boldsymbol{D}_k \cdot u_k + \nu_k, \\ z_k = \boldsymbol{\iota}_k \cdot \boldsymbol{x}_k \end{cases} \tag{18}$$

where z_k represents the vector to be estimated, $\boldsymbol{\iota}_k$ is a custom matrix. The aim is to estimate the state at each working time, in that case, $\boldsymbol{\iota}_k$ is the identity matrix which makes $z_k = \boldsymbol{x}_k$.

The core idea of HIf is to seek a balance between the disturbance and the estimator to achieve optimal estimation witha cost function J defined as follows:

$$J = \frac{\sum_{k=0}^{N-1} \|\boldsymbol{x}_k - \hat{\boldsymbol{x}}_k\|^2_{\boldsymbol{S}_k}}{\|\boldsymbol{x}_0 - \hat{\boldsymbol{x}}_0\|^2_{\boldsymbol{P}_0^{-1}} + \sum_{k=0}^{N-1}(\|\boldsymbol{\omega}_k\|^2_{\boldsymbol{Q}_k^{-1}} + \|\boldsymbol{\nu}_k\|^2_{\boldsymbol{R}_k^{-1}})} \tag{19}$$

where N represents total time of system sampling, $\boldsymbol{x}_k$ and $\hat{\boldsymbol{x}}$ represent true value and estimated value at time k, respectively, $\boldsymbol{P}_0$, $\boldsymbol{Q}_k$, $\boldsymbol{R}_k$ and $\boldsymbol{S}_k$ are symmetric positive definite matrices,

$$\begin{cases} \sum_{k=0}^{N-1} \|\boldsymbol{\omega}_k\|^2_{\boldsymbol{Q}_k^{-1}} < \infty \\ \sum_{k=0}^{N-1} \|\boldsymbol{\nu}_k\|^2_{\boldsymbol{R}_k^{-1}} < \infty \end{cases} \tag{20}$$

By adding a performance boundary δ and rearranging the Eq. (19), we have:

$$J_1 = -\frac{1}{\delta}\|\boldsymbol{x}_0 - \hat{\boldsymbol{x}}_0\|^2_{\boldsymbol{P}_0^{-1}} + \sum_{k=0}^{N-1}(\|\boldsymbol{x}_k - \hat{\boldsymbol{x}}_k\|^2_{\boldsymbol{S}_k} - \frac{1}{\delta}(\|\boldsymbol{\omega}_k\|^2_{\boldsymbol{Q}_k^{-1}} + \|\boldsymbol{\nu}_k\|^2_{\boldsymbol{R}_k^{-1}})) < 0 \tag{21}$$

The HIf algorithm is summarized as follows:

$$\hat{\boldsymbol{x}}_{k/k-1} = \boldsymbol{A}_{k-1}\hat{\boldsymbol{x}}_{k-1/k-1} + \boldsymbol{B}_{k-1}u_{k-1} \tag{22}$$

$$\boldsymbol{P}_{k/k-1} = \boldsymbol{A}_{k-1}\boldsymbol{P}_{k-1/k-1}\boldsymbol{A}_{k-1}^T + \boldsymbol{Q}_{k-1} \tag{23}$$

$$\boldsymbol{H}_k = \boldsymbol{A}_k\boldsymbol{P}_{k/k-1}[\boldsymbol{I} - \delta\boldsymbol{S}_k\boldsymbol{P}_{k/k-1} + \boldsymbol{C}_k^T\boldsymbol{R}_k^{-1}\boldsymbol{C}_k\boldsymbol{P}_{k/k-1}]^{-1}\boldsymbol{C}_k^T\boldsymbol{R}_k^{-1} \tag{24}$$

$$\hat{\boldsymbol{x}}_{k/k} = \hat{\boldsymbol{x}}_{k/k-1} + \boldsymbol{H}_k(y_k - \hat{y}_{k/k-1}) \tag{25}$$

$$\boldsymbol{P}_{k/k} = \boldsymbol{P}_{k/k-1}[\boldsymbol{I} - \delta\boldsymbol{S}_k\boldsymbol{P}_{k/k-1} + \boldsymbol{C}_k^T\boldsymbol{R}_k^{-1}\boldsymbol{C}_k\boldsymbol{P}_{k/k-1}]^{-1}, \tag{26}$$

where $\hat{\boldsymbol{x}}_{k/k-1}$ and $\boldsymbol{P}_{k/k}$ are updated state and updated covariance matrix, respectively, $\boldsymbol{H}_k$ is a filter which can

adjust prior state estimation and $\boldsymbol{S}_k$ is a third-order matrix which needs to be designed according to importance of each state. The following condition must be satisfied to make sure there's a solution at each time:

$$\boldsymbol{P}_{k/k-1}^{-1} - \delta \boldsymbol{S}_k + \boldsymbol{C}_k^T \boldsymbol{R}_k^{-1} \boldsymbol{C}_k > 0. \tag{27}$$

The HIf algorithm in Eqs. (22)–(26) can effectively estimate SOC of time-varying nonlinear lithium-ion battery system, and the estimation results are not affected by initial values, however, higher accuracy is still required and investigated. In this paper, a DSMO is integrated into the H-infinity filter which guarantees the robustness and SOC estimation accuracy.

DSMO-based H-Infinity Filter

A DSMO [46, 47] is added to the state equation in Eq. (17) as follows:

$$\begin{cases} \hat{\boldsymbol{x}}_k = \boldsymbol{A}_{k-1}\hat{\boldsymbol{x}}_{k-1} + \boldsymbol{B}_{k-1}u_{k-1} + \boldsymbol{L}(y_{k-1} - \hat{y}_{k-1}) \\ \quad + \boldsymbol{M}\text{sat}(\dfrac{y_{k-1} - \hat{y}_{k-1}}{\phi}) \\ \hat{y}_k = \boldsymbol{C}_k\hat{\boldsymbol{x}}_k + D_k u_k \end{cases} \tag{28}$$

$$\text{sat}(\mu) = \begin{cases} \mu, & -1 < \mu < 1 \\ \text{sgn}(\mu), & \mu < -1 \; or \; \mu > 1 \end{cases} \tag{29}$$

where $\boldsymbol{L}$ is the gain matrix of the observer, sat$(\cdot)$ is the saturation function with gain $\boldsymbol{M}$, ϕ as the boundary layer and sgn$(\cdot)$ the symbolic function.

The error dynamics $\tilde{\boldsymbol{x}} = \boldsymbol{x} - \hat{\boldsymbol{x}}$ can be described as follows:

$$\begin{aligned} \tilde{\boldsymbol{x}}_k &= [\boldsymbol{A} - \boldsymbol{LC}]\tilde{\boldsymbol{x}}_{k-1} + \boldsymbol{\omega}_{k-1} + \boldsymbol{L}\boldsymbol{v}_{k-1} \\ &\quad -\boldsymbol{M}\text{sat}(\frac{\boldsymbol{C}\tilde{\boldsymbol{x}}_{k-1} + v_{k-1}}{\phi}) \end{aligned} \tag{30}$$

$$\begin{aligned} &= [\boldsymbol{A} - \boldsymbol{LC}]\tilde{\boldsymbol{x}}_{k-1} + \Delta_{k-1} \\ &\quad -\boldsymbol{M}\text{sat}(\frac{C\tilde{\boldsymbol{x}}_{k-1} + v_{k-1}}{\phi}) \end{aligned} \tag{31}$$

where $\Delta_{k-1} = \boldsymbol{\omega}_{k-1} + \boldsymbol{L}\boldsymbol{v}_{k-1}$.

The stability of HIf is improved by adding a DSMO which provides a more accurate estimate for the estimated state of the HIf. Equations (22)–(26) and (28) consist of the improved HIf (IHIf) algorithm, and the Pseudo codes are shown in Algorithm 1. The framework of IHIf with parameter identification algorithm FFRLS is shown in Fig. 2. The stability analysis of the modified algorithm is shown in Ref. [48].

Algorithm 1 IHIf algorithm.

Input: $\hat{\boldsymbol{x}}_{k-1/k-1}$, $\boldsymbol{P}_{k-1/k-1}$, $length$
Output: $\hat{\boldsymbol{x}}_{k/k}$, $\boldsymbol{P}_{k/k}$
1: Initialization: $\hat{\boldsymbol{x}}_{0/0} = [1, 0, 0]^{\mathrm{T}}$, $\boldsymbol{P}_{0/0} = \boldsymbol{I}_3$, $\boldsymbol{Q} = 10^{-8}\boldsymbol{I}_3$, $R = 10^{-1}$
2: $k = 1$
3: **while** $k < length$ **do**
4: State estimate: $\hat{\boldsymbol{x}}_{k/k-1} = \boldsymbol{A}_{k-1}\hat{\boldsymbol{x}}_{k-1/k-1} + \boldsymbol{B}_{k-1}\boldsymbol{u}_{k-1} + \boldsymbol{L}(\boldsymbol{y}_{k-1} - \hat{\boldsymbol{y}}_{k-1}) + \boldsymbol{M} \cdot sat(\frac{\boldsymbol{y}_{k-1} - \hat{\boldsymbol{y}}_{k-1}}{\phi})$
5: State estimate covariance $\boldsymbol{P}_{k/k-1} = \boldsymbol{A}_{k-1}\boldsymbol{P}_{k-1/k-1}\boldsymbol{A}_{k-1}^T + \boldsymbol{Q}_{k-1}$
6: Gain update $\boldsymbol{H}_k = \boldsymbol{A}_k\boldsymbol{P}_{k/k-1}[\boldsymbol{I} - \delta\boldsymbol{S}_k\boldsymbol{P}_{k/k-1} + \boldsymbol{C}_k^T\boldsymbol{R}_k^{-1}\boldsymbol{C}_k\boldsymbol{P}_{k/k-1}]^{-1}\boldsymbol{C}_k^T\boldsymbol{R}_k^{-1}$
7: Update state estimate $\hat{\boldsymbol{x}}_{k/k} = \hat{\boldsymbol{x}}_{k/k-1} + \boldsymbol{H}_k(\boldsymbol{y}_k - \hat{\boldsymbol{y}}_{k-1})$
8: State covariance $\boldsymbol{P}_{k/k} = \boldsymbol{P}_{k/k-1}[\boldsymbol{I} - \delta\boldsymbol{S}_k\boldsymbol{P}_{k/k-1} + \boldsymbol{C}_k^T\boldsymbol{R}_k^{-1}\boldsymbol{C}_k\boldsymbol{P}_{k/k-1}]^{-1}$
9: $k = k + 1$
10: **end while**

Experiments and analysis

To verify the accuracy of the IHIf algorithm in SOC estimation, two experiments of discharge test and DST are conducted. DST is a simplified version of Federal Urban Driving Schedule, which is one of the most commonly operating conditions of the simulation vehicle. DST experiments simulate the actual operation of electric vehicles through load curves. The charge-discharge current of one cycle is shown in Fig. 7(b) and the experiment cycle is completed until the battery voltage drops to the cut-off voltage. Referring to Fig. 3, the battery experiment platform is used to detect the Li(NiCoMn)O2 material LiBs cell at room temperature (25 °C) which includes a host computer, a multi-range battery tester (NEWARE CT-4008), Samsung ICR18650 (2600 mAh) LiBs, and a battery clamp. The details of the LiBs are shown in Table 1.

The structure and test flow chart of the battery test system are shown in Fig. 4. Table 2 and Fig. 5 show the fitting relationship between OCV and SOC, which can be identified by battery intermittent charging and discharging experiments.

Consider the system stability analysis and computational complexity, set the initial SOC is 1, δ is 10^4 and $\boldsymbol{S_k}$ is the third-order identity matrix, respectively, ϕ =0.1, $\boldsymbol{L}$ = [2 $*$ 10^{-5}; -0.5; -0.5], $\boldsymbol{M}$=[10^{-6}; 0.001; 0.001], $\boldsymbol{Q}_0 = 10^{-8}\boldsymbol{I}_3$, and $R = 0.1$.

In the intermittent discharge experiment, the discharge current is negative. Results under intermittent constant

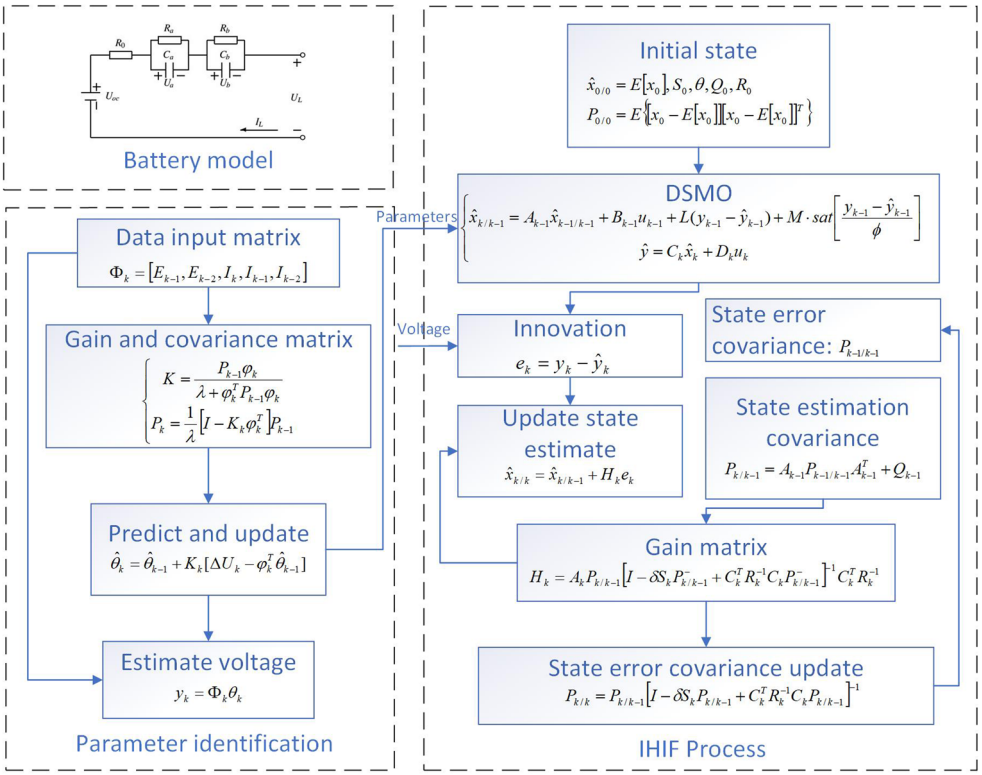

Fig. 2 Lithium-ion battery identification and estimation process

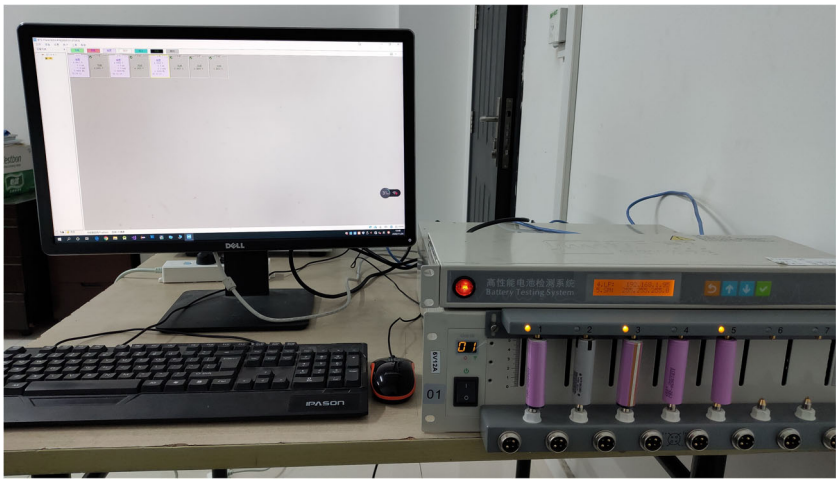

Fig. 3 The battery test platform

Table 1 Specification of Samsung ICR18650

Capacity	2600mAh
Normal voltage	3.63V
Min/max voltage	2.75V/4.2V
Standard charge/rapid charge	1.3A/2.6A
Max charge current	2.6A
Max discharge current	5.2A
Discharge temperature	− 20 °C/60 °C
Dimensions	18.00*65.00mm

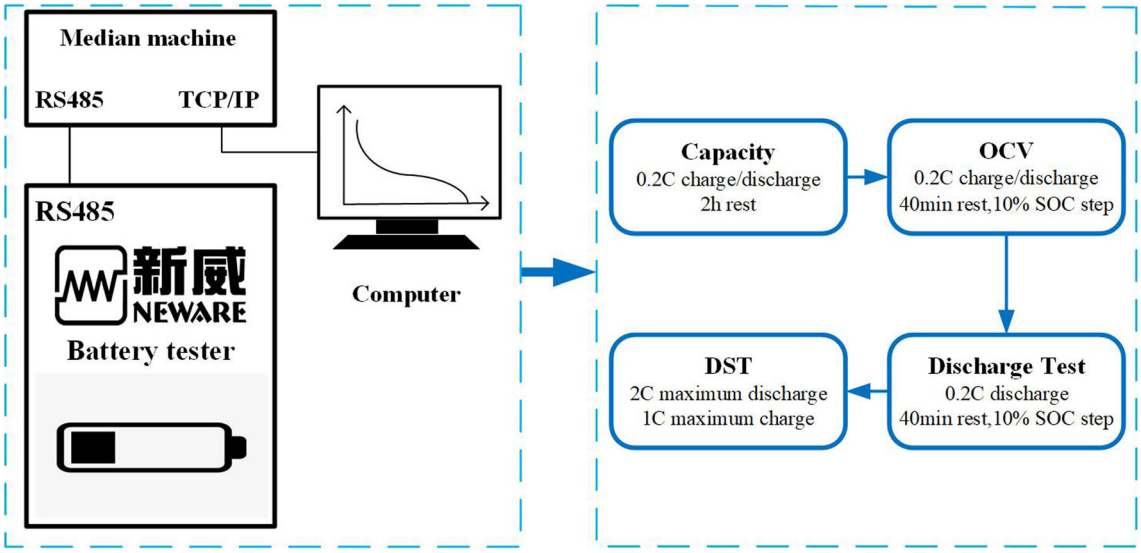

Fig. 4 Flowchart of the battery tests

Table 2 The relation between OCV and SOC

SOC	1	0.9	0.8	0.7	0.6	0.5	0.4	0.3	0.2	0.1	0
OCV(Charge)	4.1905	3.9946	3.8950	3.8051	3.7379	3.6644	3.6328	3.6077	3.5773	3.4936	3.4058
OCV(Discharge)	4.1548	4.029	3.9211	3.8234	3.7419	3.6662	3.6272	3.5993	3.5667	3.4833	3.4000

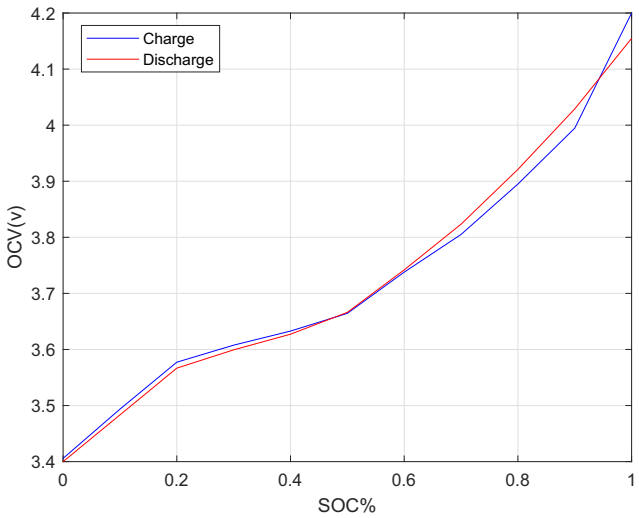

Fig. 5 The relation between OCV and SOC under charge and discharge test

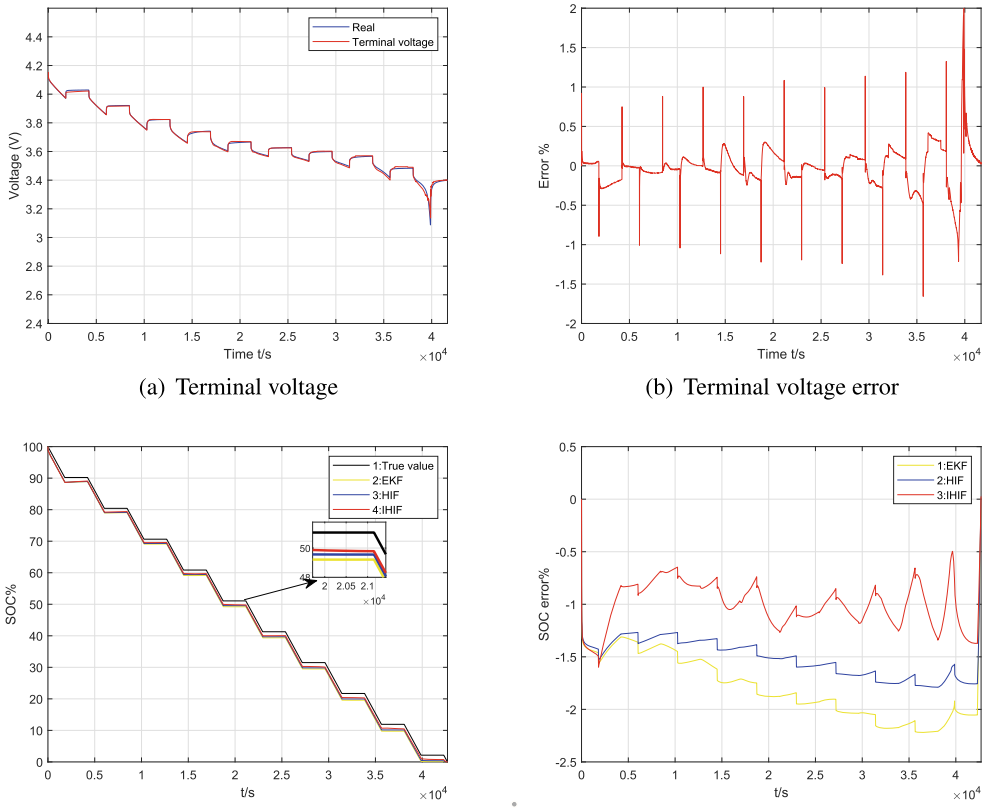

(a) Terminal voltage

(b) Terminal voltage error

(c) State of charge

(d) State of charge error

Fig. 6 The error of SOC estimation under intermittent discharge test

current condition are shown in Fig. 6, where the comparison between the proposed method IHIf and other methods are shown in Fig. 6(c) and (d) and the Mean Absolute Error (MAE) and Root Mean Square Error (RMSE) of the EKF, HIf and IHIf are in Table 3. From Fig. 6(c), (d) and Table 3, the estimated SOC by IHIf is close to the true SOC and has smaller error.

Consider the real operating environment of LiBs in electric vehicles, the LiBs working condition of the test data is sampled under DST conditions. It can be seen that the terminal voltage and the state-of-charge curve fluctuate with the multiple discharge and charging processes of the incoming line current, and the stability is lower than that under constant current conditions. The battery's DST current profile and voltage profile are illustrated in Fig. 7(a) and (c). Figure 7(b) is a single cycle of DST. The error of the voltage estimation of the method is shown in Fig. 7(d).

Table 3 Comparison on estimation error of SOC under discharge test

Algorithm	EKF	HIf	IHIf
MAE	1.7955	1.5182	1.0031
RMSE	1.8213	1.5296	1.0257

The EKF, HIf and the IHIf algorithm are applied to SOC estimation in Fig. 7(e) and (f). The MAE and RMSE of the EKF, HIf and IHIf are listed in Table 4. Consider complex charge and discharge condition in dynamic stress test, both HIf and IHIf algorithm can estimate SOC under different conditions; however, the latter has better robustness and improves the estimation accuracy.

Although it is verified that the proposed algorithm improves accuracy and stability, it does not bring extra computations. A comparison of calculation cost was performed on a 1.1GHz Intel Core i7-10710U processor and 16.0GB memory. Since the execution process of the algorithm's Matlab script is affected by the state of the PC's CPU and memory, 50 experiments were carried out in the same state of the computer to verify the time spent by the algorithm. Table 5 shows the average computation times under different methods.

From Table 5, the computational time of IHIf increases by 14.4% and 2.8% under discharge test compared to that of EKF and HIf and increases by 7.6% and 0.99% under DST, which means that the IHIf has improved accuracy without bringing in calculation burden.

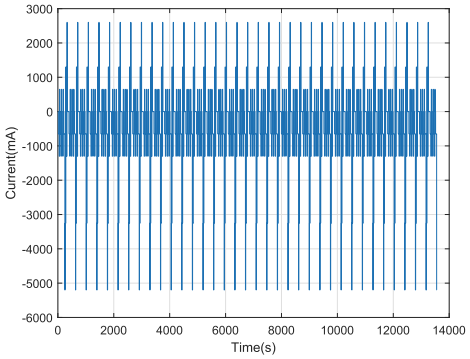

(a) Dynamic stress test (DST) profiles

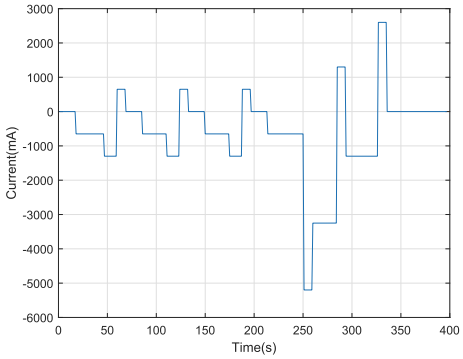

(b) DST (1 cycle)

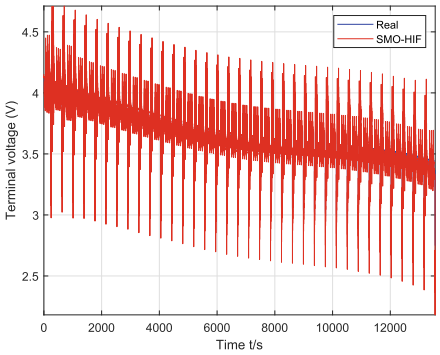

(c) Terminal voltage

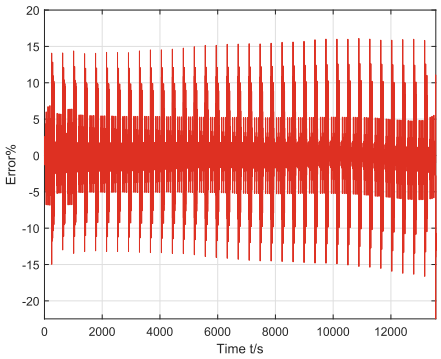

(d) Terminal voltage error

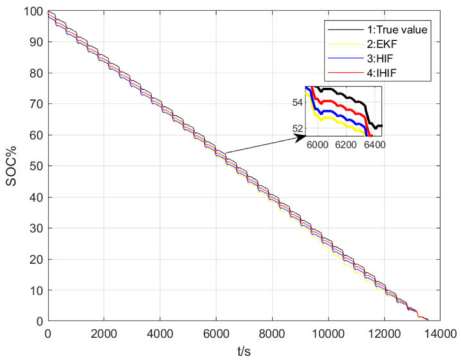

(e) The SOC estimation under DST

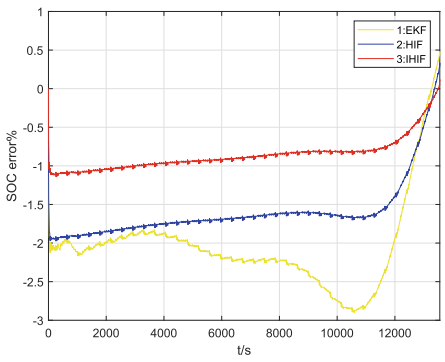

(f) The error of SOC estimation under DST

Fig. 7 The SOC estimation under DST

Table 4 Comparison on estimation error of SOC under DST

Algorithm	EKF	HIf	IHIf
MAE	2.0546	1.6036	0.8615
RMSE	2.1282	1.6451	0.8856

Table 5 Computation time under different methods

Algorithm	EKF	HIf	IHIf
Discharge test (s)	0.4374	0.4862	0.5002
DST (s)	0.9361	0.9973	1.0072

Conclusions

In this paper, an H-infinite filtering combined with DSMO is proposed to estimate SOC. The proposed method aims to improve the robustness and accuracy of the estimation. Discharge test and DST results prove that the IHIf algorithm can accurately estimate SOC, and the accuracy is better than EKF and HIf. To better estimate SOC, model selection and algorithm improvement are the focus of future research.

Funding This work was supported by Natural Science Foundation of Jangsu Province and the Natural Science Foundation of NJUPT under Grant NY220217.

References

1. Zhang C, Yang F, Ke XY, Liu ZF, Yuan C (2019) Predictive modeling of energy consumption and greenhouse gas emissions from autonomous electric vehicle operations. Appl Energy 254:113597
2. Saha P, Dey S, Khanra M (2020) Modeling and State-of-Charge Estimation of Supercapacitor Considering Leakage Effect. IEEE Trans on Ind Electron 67:350–357
3. Berecibar M, Gandiaga I, Villarreal I, Omar N, Mierlo JV, Bossche PVD (2016) Critical review of state of health estimation methods of Li-ion batteries for real applications. Renew Sustain Energy Rev 56:572–587
4. Hannan MA, Lipu MSH, Hussain A, Mohamed A (2017) A review of lithium-ion battery state of charge estimation and management system in electric vehicle applications: challenges and recommendations. Renew Sustain Energy Rev 78:834–854
5. Wang YB, Fang HZ, Zhou L, Wada T (2017) Revisiting the state-of-charge estimation for lithium-ion batteries: A methodical investigation of the extended Kalman filter approach. IEEE Contr Syst 37:73–96
6. Li XY, Wang ZP, Zhang L (2019) Co-estimation of capacity and state-of-charge for lithium-ion batteries in electric vehicles. Energy 174:33–44
7. Xiong R, Tian JP, Mu H, Wang C (2017) A systematic model-based degradation behavior recognition and health monitoring method for lithium-ion batteries. Appl Energy 207:372–383
8. Zheng FD, Xing YJ, Jiang JC, Sun BX, Kim J, Pecht M (2016) Influence of different open circuit voltage tests on state of charge online estimation for lithium-ion batteries. Appl Energy 183:513–525
9. Hu XS, Jiang HF, Feng F, Liu B (2020) An enhanced multi-state estimation hierarchy for advanced lithium-ion battery management. Appl Energy 257:114019
10. Ghalkhani M, Bahiraei F, Nazi GA, Saif M (2017) Electro-chemicaleThermal model of pouch-type lithium-ion batteries. Electrochim Acta 247:569–587
11. Wang QK, He YJ, Shen JN, Ma ZF, Zhong GB (2017) A unified modeling framework for lithium-ion batteries: an artificial neural network based thermal coupled equivalent circuit model approach. Energy 138:118–132
12. Jiao M, Wang DQ, Qiu LJ (2020) GRU-RNN based momentum optimized algorithm for SOC estimation. J Power Sources 459:228051
13. Chemali E, Kollmeyer PJ, Preindl M, Ahmed R, Emadi A (2018) Long short-term memory networks for accurate state-of-charge estimation of Li-ion batteries. IEEE Trans Ind Electron 65:6730–6739
14. Sheng H, Xiao J (2015) Electric vehicle state of charge estimation: nonlinear correlation and fuzzy support vector machine. J Power Sources 281:131–137
15. Xia B, Cui D, Sun Z, Lao Z, Zhang R, Wang W (2018) State of charge estimation of lithium-ion batteries using optimized Levenberg-Marquardt wavelet neural network. Energy 153:694–705
16. Moura S, Chaturvedi N, Krstic M (2012) PDE estimation techniques for advanced battery management systems; Part I: SOC estimation. Am Control Conf 2012:559–565
17. Klein R, Chaturvedi N, Christensen J, Ahmed J, Findeisen R, Kojic A (2013) Electrochemical model based observer design for a lithiumion battery. IEEE Trans Contr Syst Technol 21:289–301
18. Tran N, Vilathgamuwa D, Li Y, Farrell TW, Choi SS, Teague J (2017) State of charge estimation of lithium ion batteries using an extended single particle model and sigma-point Kalman1 filter. In: IEEE southern power electronics conference, vol 2017, pp 624–629
19. Yang JF, Huang W, Xia B, Mi C (2019) The improved open-circuit voltage characterization test using active polarization voltage reduction method. Appl Energy 237:682–694
20. Shen YQ (2018) A chaos genetic algorithm based extended Kalman filter for the available capacity evaluation of lithium-ion batteries. Electrochim Acta 264:400–409
21. Zhang LJ, Peng H, Ning ZS, Mu ZQ, Sun CY (2017) Comparative research on RC equivalent circuit models for lithium-ion batteries of electric vehicles. Appl Sci 7:1002
22. Dai HF, Wei XZ, Sun ZC, Wang JY, Gu WJ (2012) Online cell SOC estimation of Li-ion battery packs using a dual time-scale Kalman filtering for EV applications. Appl Energy 95:227–237
23. He HW, Qin HZ, Sun XK, Shui YP (2013) Comparison study on the battery SoC estimation with EKF and UKF algorithms. Energies 6:5088–5100
24. Ramadan H, Becherif M, Claude F (2017) Extended Kalman filter for accurate state of charge estimation of lithium-based batteries: a comparative analysis. Int J Hydrogen Energy 42:29033–29046
25. Xu J, Mi CC, Cao BG, Deng JJ, Chen ZZ, Li S (2014) The state of charge estimation of lithium-ion batteries based on a proportional-integral observer. IEEE Trans Veh Technol 63:1614–1621
26. Chen XP, Shen WX, Cao ZW, Kapoor A (2014) A novel approach for state of charge estimation based on adaptive switching gain sliding mode observer in electric vehicles. J Power Sources 2469:667–678
27. Chen S, Fu YH, Mi C (2013) State of charge estimation of lithium-ion batteries in electric drive vehicles using extended Kalman filtering. IEEE Trans Veh Technol 62:1020–1030
28. Wang YJ, Zhang CB, Chen ZH (2015) A method for state-of-charge estimation of Li-ion batteries based on multi-model switching strategy. Appl Energy 137:427–434
29. Perez G, Garmendia M, Reynaud JF, Crego J, Viscarret U (2015) Enhanced closed loop State of Charge estimator for lithium-ion batteries based on Extended Kalman Filter. Appl Energy 155:834–845
30. Li WQ, Yang Y, Wang DQ, Yin SQ (2020) The multi-innovation extended Kalman filter algorithm for battery SOC estimation. Ionics 26:6145–6156
31. Zhu Q, Li L, Hu XS, Xiong N, Hu G (2017) H∞-based nonlinear observer design for state of charge estimation of lithium-ion battery with polynomial parameters. IEEE Trans Veh Technol 66:10853–10865
32. Liu Z, Dang XJ (2018) A new method for State of Charge and capacity estimation of lithium-ion battery based on dual strong tracking adaptive H-infinity filter. Math Probl Eng :5218205

33. Farmann A, Waag W, Marongiu A (2015) Critical review of on-board capacity estimation techniques for lithium-ion batteries in electric and hybrid electric vehicles. J Power Sources 281:114–130
34. Z Wei, C Zou, F Leng, BH Soong, KJ Tseng (2018) Online model identification and state-ofcharge estimate for lithium-ion battery with a recursive total least squares-based observer. IEEE Trans Ind Electron 65:1336–1346
35. Chen XK, Lei H, Xiong R, Shen WX, Yang R (2019) A novel approach to reconstruct open circuit voltage for state of charge estimation of lithium ion batteries in electric vehicles. Appl Energy 255:113758
36. Luo JY, Peng JK, HE HW (2019) Lithium-ion battery SOC estimation study based on Cubature Kalman filter. Energy Procedia 158:3421–3426
37. Lao ZZ, Xia BZ, Wang W, Sun W, Lai Y, Wang M (2018) A novel method for lithium-ion battery online parameter identification based on variable forgetting factor recursive least squares. Energies 11:1358
38. Claude F, Becherif M, Ramadan HS (2017) Experimental validation for Li-ion battery modeling using Extended Kalman Filters. Int J Hydrogen Energy 42:25509–25517
39. Feng L, Ding J, Han YY (2020) Improved sliding mode based EKF for the SOC estimation of lithium-ion batteries. Ionics 26:2875–2882
40. Chen QY, Jiang JC, Ruan HJ (2017) Simply designed and universal sliding mode observer for the SOC estimation of lithium-ion batteries. IET Power Electron 10:697–705
41. Hu XS, Li SB, Peng H (2012) A comparative study of equivalent circuit models for Li-ion batteries. J Power Sources 198:359–367
42. Zhu R, Duan B, Zhang J, Zhang Q, Zhang Q (2020) Co-estimation of model parameters and state-of-charge for lithium-ion batteries with recursive restricted total least squares and unscented Kalman filter. Appl Energy 277:115494
43. Constantin P, Jacob B, Silviu C (2008) A robust variable forgetting factor recursive least-squares algorithm for system identification. IEEE Signal Process Lett 15:597–600
44. Li XL, Zhou LC, Sheng J (2014) Recursive least squares parameter estimation algorithm for dual-rate sampled-data nonlinear systems. Nonlinear Dyn 76:1327–1334
45. Sun F, Xiong R (2015) A novel dual-scale cell state-of-charge estimation approach for series-connected battery pack used in electric vehicles. J Power Sources 274:582–594
46. Thein MWL (2003) A discrete time variable structure observer for uncertain systems with measurement noise. In: Proc. IEEE conference on decision and control, vol 2003, pp 2582–2587
47. Harikumar K, Bera T, Bardhan R (2019) Discrete-time sliding mode observer for the state estimation of a manoeuvring target. J Syst Contr Eng 233:095965181982648
48. Thein MWL (2002) A discrete time variable structure observer with overlapping boundary layers. In: Proc. Amer Control Conf, pp 2633–2638